JACS
JOURNAL OF THE AMERICAN CHEMICAL SOCIETY

Communication

pubs.acs.org/JACS

Dual-Time Scale Photoinduced Electron Transfer from PbS Quantum Dots to a Molecular Acceptor

Kathryn E. Knowles, Michał Malicki, and Emily A. Weiss*

Department of Chemistry, Northwestern University, 2145 Sheridan Road, Evanston, Illinois 60208-3113, United States

Supporting Information

ABSTRACT: A combination of picosecond and microsecond transient absorption dynamics reveals the involvement of two mechanisms by which 1,4-benzoquinone (BQ) induces the decay of the excited state of PbS quantum dots (QDs): (i) electron transfer to BQ molecules adsorbed to the surfaces of PbS QDs and (ii) collisionally gated electron transfer to freely diffusing BQ. Together, these two mechanisms quantitatively describe the quenching of photoluminescence upon addition of BQ to PbS QDs in dichloromethane solution. This work represents the first quantitative study of a QD−ligand system that undergoes both adsorbed and collisionally gated photoinduced charge transfer within the same sample. The availability of a collisionally gated pathway improves the yield of electron transfer from PbS QDs to BQ by an average factor of 2.5 over that for static electron transfer alone.

This paper describes the mechanisms by which both adsorbed and freely diffusing 1,4-benzoquinone (BQ) molecules accept electrons from the lowest-energy excitonic state of solution-phase PbS quantum dots (QDs). We quantitatively separate the contributions of static and collisionally gated photoinduced electron transfer (PET) to total excitonic decay through transient absorption (TA) experiments that monitor the dynamics of the ground-state bleach feature of the QDs on picosecond and microsecond time scales, respectively. PbS QDs absorb in the near-infrared, and have greater carrier multiplication efficiencies[1−3] and longer excited-state lifetimes[4−6] than CdSe or CdS QDs. These properties make PbS QDs potentially more attractive for photovoltaic or photocatalytic applications than CdSe or CdS QDs because (i) they absorb a greater fraction of the solar spectrum, (ii) they can produce multiple charge carriers for each absorbed photon with higher yields, and (iii) their longer exciton lifetime allows them more time to donate an electron or hole to a redox partner. In fact, as we demonstrate here, the exciton lifetime of PbS QDs (~2.6 μs) is long enough for the QD to participate in collisionally gated charge transfer with a diffusing molecule, in addition to exchanging electrons with molecules adsorbed at the time of photoexcitation (Figure 1), a property that potentially enhances the yield of photocurrent generation in a photoelectrochemical cell.[7] This work provides a framework for understanding charge transfer not only between QDs and bound ligands—a problem that has been treated extensively in the context of Marcus parameters (driving force and donor/acceptor distance)[8−10]—but also between QDs and freely diffusing molecules.

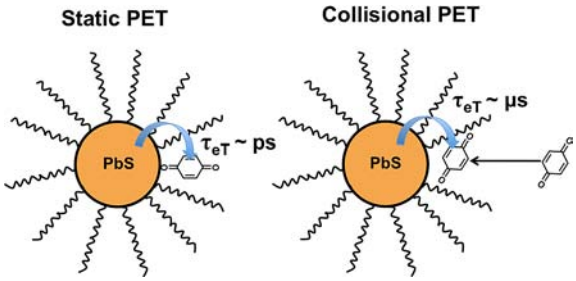

Figure 1. Two mechanisms of photoinduced electron transfer from a PbS quantum dot to 1,4-benzoquinone. (Left) Static PET from a PbS QD to an adsorbed BQ molecule. (Right) Collisional PET between a QD with no adsorbed BQ ligands and a freely diffusing BQ molecule.

We use a procedure adapted from that of Hines and Scholes to synthesize PbS QDs with an average diameter of 3.4 ± 0.3 nm (see Supporting Information (SI)).[11] These QDs have a band-edge absorption peak centered at 967 nm and a photoluminescence (PL) peak centered at 1095 nm (see SI). We added various amounts of BQ to a stock solution of PbS QDs to create a series of samples that contained the same concentration of QDs but different concentrations of BQ, and performed TA and PL measurements on these solutions within 6 h of their preparation. We chose BQ as the electron acceptor because (i) Burda et al. previously observed PET from CdSe QDs to adsorbed BQ;[12] (ii) based on the reduction potential of BQ and the energy of the conduction band-edge of a 3.4-nm PbS QD, PET from PbS QDs to BQ has $\Delta G = -0.3$ eV (see SI); and (iii) neutral ligands, like BQ, that bind to QD surfaces via donation of oxygen lone pairs are weak adsorbers.[13] Mixtures of QDs and such ligands contain an appreciable population of QDs with no adsorbed ligands even at high ligand concentrations.

Figure 2A shows a TA spectrum of a solution of PbS QDs in CH_2Cl_2 at 1 ps after 930-nm photoexcitation. The negative feature centered at 930 nm is the bleach of the ground-state band-edge absorption of the QDs (GS bleach). Removal of either electron or hole population from the $1S_e$-$1S_h$ excitonic state of PbS QDs by charge transfer, charge trapping, or radiative recombination results in the recovery of the GS bleach.[9,14] Figure 2B,C shows kinetic traces extracted from the GS bleach feature within the TA spectra of a series of solutions

Received: June 20, 2012
Published: July 19, 2012

   dx.doi.org/10.1021/ja3060222 | J. Am. Chem. Soc. 2012, 134, 12470−12473

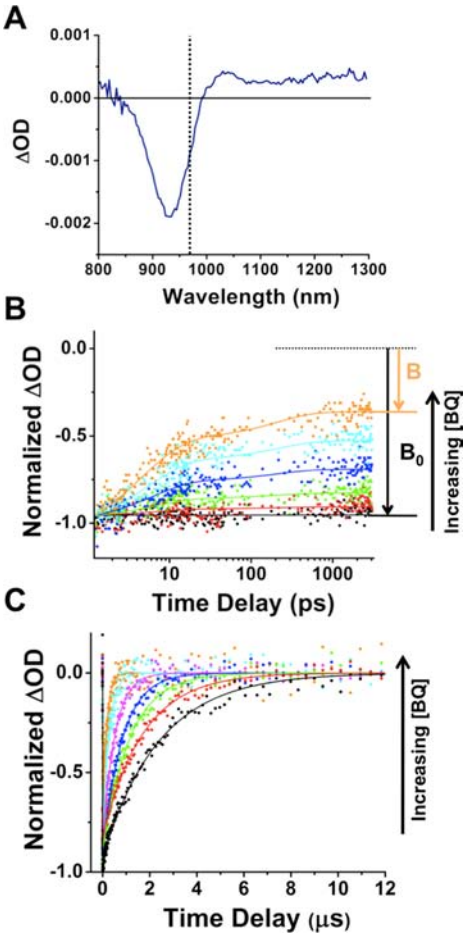

Figure 2. (A) Transient absorption spectrum of a solution of 3.4-nm PbS QDs in CH_2Cl_2 acquired 1 ps after excitation with a 930-nm pump pulse. The vertical dotted line indicates the probe wavelength (965 nm) at which kinetic traces were recorded to determine the dynamics of exciton decay. (B,C) Normalized kinetic traces on the ps (B) and μs (C) time scales, at a probe wavelength of 965 nm, from TA spectra of a solution of PbS QDs (black trace) and solutions of PbS QDs and various concentrations of added BQ, ranging from 0.34 to 11 mM (colored traces). The solid lines are fits of the kinetic traces; the fit functions are explained in the text. The lifetime of the exciton without added BQ is 2.6 μs (see fit indicated by black line in C), and decreases with increasing [BQ] on both time scales.

of PbS QDs with various concentrations of added BQ on the ps and μs time scales, respectively. The dynamic traces on both time scales show that the first excitonic state of the PbS QDs decays more quickly with increasing [BQ].

We attribute the acceleration of excitonic decay by BQ to PET from the conduction band-edge of the QD to the LUMO of BQ. We eliminate energy transfer as a cause of exciton decay because BQ does not exhibit any absorption features at wavelengths longer than 950 nm, the shortest wavelength at which the QDs emit (see SI).

We observe cross-coupling signals corresponding to protons within the oleate ligand shell of the QDs upon selective excitation of BQ protons in a 1D-NOESY NMR experiment (see SI); this observation indicates that some fraction of BQ molecules are adsorbed to the surfaces of QDs.[15] We suspect that BQ adsorbs to QDs through one of the oxygen lone pairs (Figure 1). Given this result, and the fast (ps) time scale of the PET processes responsible for the kinetic traces in Figure 2B, we conclude that these PET processes occur from QDs to adsorbed BQ ligands. The equilibrium constant, K_a, for adsorption of BQ to PbS QDs is 200 M^{-1} (see SI).

Under low fluence (average number of photons absorbed per QD, $\langle N \rangle \leq 0.3$), where the probability of formation of multiexciton states through multiphoton absorption is $\lesssim$3%, there is no decay of the PbS QD excited state on the ps time scale (black trace in Figure 2B). Addition of BQ results in ps kinetic traces that we fit to a function (eq 1) comprising three decay components: (i) Poisson-distributed charge separation (CS) via PET from photoexcited QDs to adsorbed BQs, where $k_{CS,int}$ is the intrinsic CS rate constant for a QD with one adsorbed BQ;[15,16] (ii) charge recombination (CR) with rate constant k_{CR}; and (iii) a long decay component that corresponds to the μs dynamics shown in Figure 2C.

$$\Delta OD(t) = -[A_{CS}\, e^{-\lambda}(\exp(\lambda\, e^{-k_{CS,int}t}) - 1) + A_{CR}(1 - e^{-\lambda})e^{-k_{CR}t} + e^{-\lambda}e^{-t/\tau_{\mu s}}] \quad (1)$$

In eq 1, $\tau_{\mu s}$ is the time constant for excitonic decay on the μs time scale measured from single-exponential fits of the kinetic traces in Figure 2C, A_{CS} and A_{CR} account for the relative contribution of the electron and hole, respectively, to the total amplitude of the bleach, and λ is the average number of BQ molecules adsorbed per QD, given by the Poisson distribution. Using a method we described previously,[16] we fix the value of λ to $-\ln(B/B_0)$ for each trace, where B/B_0 is the fraction of QDs with zero adsorbed BQ ligands. We measure B/B_0 as the ratio of the average bleach amplitude at delay times of 2500−3000 ps (well after CR) for samples of QDs with (B) and without (B_0) added BQ. The SI contains a detailed derivation of eq 1.

We apply eq 1 in a global fit of the ps kinetic traces for bleach recovery (Figure 2B, see SI). In this global fit, $k_{CS,int}$ and k_{CR} are shared among all of the traces because these quantities, by definition, are independent of [BQ]. The parameters A_{CS} and A_{CR} are also shared among all of the traces in the global fit because the dependence of the fractional amplitudes of the CS and CR components on [BQ] is accounted for by the terms that contain λ ($e^{-\lambda}$, $1 - e^{-\lambda}$).

The average values of $k_{CS,int}$ and k_{CR} obtained from globally fitting three different sets of ps time scale dynamics—acquired on separate days from three different series of samples—to eq 1 are $(2.6 \pm 1.2) \times 10^{11}$ and $(1.1 \pm 0.8) \times 10^{10}$ s^{-1}, respectively. One of the sample series contained QDs from a different synthetic batch than the other two sample series; batch-to-batch variations in surface structure and/or initial coverage of the oleate native ligand[17] probably account for the variation in values for $k_{CS,int}$ and k_{CR}.

Dynamics of GS bleach recovery on the μs time scale (Figure 2C) fit to single-exponential functions with time constants, $\tau_{\mu s}$, that decrease as [BQ] increases (see SI for a table of time constants). The exciton lifetime of a solution of PbS QDs with no added BQ is $\tau_{\mu s,0} = 2.55 \pm 0.03$ μs, which is consistent with previous measurements of exciton lifetimes for PbS QDs in the range 1−3 μs.[4,5,18] The fact that the time constants $\tau_{\mu s}$ depend on [BQ] indicates that the μs dynamics correspond to a different CS process from that on the ps time scale. Additionally, since the bleach completely recovers on the μs time scale, the μs dynamics also include contributions from CR. The SI outlines a kinetic model for the μs dynamics that contains a [BQ]-dependent CS rate constant and a [BQ]-independent CR rate constant.

dx.doi.org/10.1021/ja3060222 | J. Am. Chem. Soc. 2012, 134, 12470−12473

There are two possible mechanisms for PET on the μs time scale: (i) PET occurs via tunneling through the oleate ligand shell from BQ molecules that are located within the ligand shell upon photoexcitation, or (ii) BQ molecules diffusing in solution collide with photoexcited QDs and some fraction of these collisions result in PET. If mechanism (i) were responsible for the PET dynamics observed on the μs time scale, we would expect to observe a range of CS rate constants corresponding to BQ molecules distributed within the ligand shell over a range of distances (up to 19 Å) from the surface of the QD. Instead, we find that, in order to produce distributions in CS rates that fit the μs traces in Figure 2C, the distributions of donor−acceptor distances for the QD−BQ systems must be less than ∼1−2 Å wide (assuming exponential attenuation of tunneling through a low-dielectric medium, see SI). It is unlikely that BQ molecules randomly distributed within the ligand shell of the QD would occupy such a narrow range of distances from the QD surface. Mechanism (i) therefore is probably not the primary pathway for μs PET.

Mechanism (ii), in which PET from PbS QDs to BQ is collisionally gated, predicts a linear Stern−Volmer plot of the μs time constants that reflects a linear dependence of the CS rate constant on [BQ]. As shown in Figure 3, the plot of the ratio $\tau_{\mu s,0}/\tau_{\mu s}$ versus [BQ] is indeed linear. Fitting this plot to eq 2, the Stern−Volmer equation for dynamic quenching of a photoexcited fluorophore,[19]

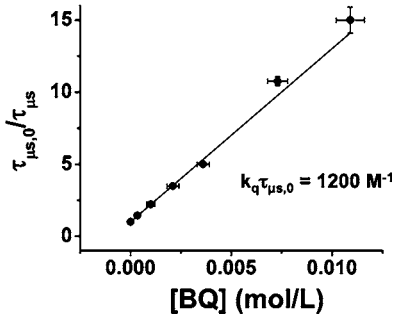

Figure 3. Plot of the ratio of the μs time constant for GS bleach recovery for a solution of PbS QDs with no added BQ ($\tau_{\mu s,0}$) to that for samples with added BQ ($\tau_{\mu s}$) versus [BQ]. These data represent error-weighted average values for four separate series of samples. The SI details the calculation of these averages and of the corresponding error bars. The solid line is the fit of the data to eq 2.

$$\frac{\tau_{\mu s,0}}{\tau_{\mu s}} = 1 + k_q\tau_{\mu s,0}[\mathrm{BQ}] \qquad (2)$$

yields a slope of $k_q\tau_{\mu s,0}$ = 1200 M^{-1}, where k_q is the bimolecular quenching constant. Dividing this slope by $\tau_{\mu s,0}$ = 2.55 μs gives $k_q = 4.7 \times 10^8$ M^{-1} s^{-1}.

This bimolecular quenching constant is more than a factor of 100 smaller than the diffusion-limited rate constant for collisional PET ($k_0 = 8.5 \times 10^{10}$ M^{-1} s^{-1}, see SI), which we calculate from diffusion constants for the QDs and BQ measured with diffusion-ordered spectroscopy (DOSY) NMR (see SI). When calculating k_0, we define the radius for a QD−BQ collision to be the sum of the radius of the core of the QD (1.7 nm), the through-space length of an oleate ligand (1.9 nm), and the radius of a BQ molecule (0.2 nm). The diffusion-limited rate constant k_0 therefore describes the rate at which a BQ molecule contacts or penetrates the outer edge of the ligand shell of a QD. The collisional quenching efficiency, k_q/k_0 = 0.006, is the fraction of collisions between BQ and the ligand shell of a photoexcited QD that result in electron transfer. We suspect that the collisional quenching efficiency is limited by the ability of BQ to diffuse to a location where the PET rate is faster than the exciton recombination rate, as determined by the permeability of the oleate ligand shell.[15]

Figure 4 (inset) shows PL spectra for a series of solutions of PbS QDs with various concentrations of added BQ. As [BQ] increases, the intensity of the QD PL peak decreases. Figure 4 shows that the product of experimentally measured values of B/B_0 (the fraction of QDs that do not participate in static PET) and $\tau_{\mu s}/\tau_{\mu s,0}$ (the fraction of QDs that do not participate in collisionally gated PET)[19] agrees well with the measured values of PL/PL$_0$ for all concentrations of added BQ studied here. This agreement implies that the ratio PL/PL$_0$ is the fraction of QDs that are not quenched by either mechanism, and that the steady-state PL response to addition of BQ is well-described by a combination of charge transfer to adsorbed BQ and collisionally gated charge transfer. Additionally, either mechanism alone cannot account for the total PL response to addition of BQ (see SI).

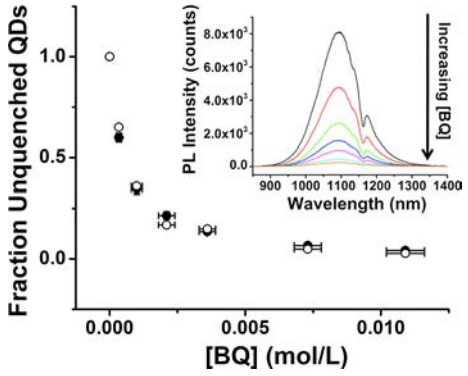

Figure 4. Plot of the ratio of the integrated PL intensity of solutions of PbS QDs with various concentrations of added BQ ("PL") to the integrated PL intensity of a solution of PbS QDs with no added BQ ("PL$_0$", solid circles) and the product $(B/B_0)(\tau_{\mu s}/\tau_{\mu s,0})$ (open circles) as a function of [BQ]. The SI shows the calculations of the error bars. (Inset) Steady-state PL spectra of a solution of PbS QDs (black) and a series of solutions of PbS QDs with concentrations of added BQ ranging from 0.34 to 11 mM (colored) in CH_2Cl_2. The "dip" in the PL spectra at 1160 nm corresponds to an absorption peak of CH_2Cl_2 (see SI).

We have demonstrated that BQ quenches the excited state of oleate-coated PbS QDs on both the ps and μs time scales (Figure 2) within the same sample. The ps dynamics monitored at the GS bleach of the QDs are due to CS and CR between photoexcited QDs and adsorbed BQ molecules (Figure 2B). The exciton quenching on the μs time scale is due to collisionally gated PET between QDs (with no adsorbed BQ molecules) and freely diffusing BQ molecules (Figure 2C). A Stern−Volmer analysis of the μs dynamics reveals that only 0.6% of QD−BQ collisions result in PET (Figure 3). Both mechanisms—charge transfer to adsorbed BQ ("static PET") and collisionally gated charge transfer ("collisional PET", Figure 1)—are required to describe the total quenching of steady-state PL of the QDs upon addition of BQ. We found that collisional PET improves the overall yield of PET from PbS QDs to BQ by a factor of 2.5 over that for static PET alone.

dx.doi.org/10.1021/ja3060222 | J. Am. Chem. Soc. 2012, 134, 12470−12473

Our demonstration of collisional PET reveals that, unlike in more commonly studied CdSe and CdS QDs, the long exciton lifetime of PbS QDs enables PET with redox partners that are not adsorbed to the QD surface. This ability eliminates the need for complex synthesis of molecular redox partners that contain surface-anchoring groups, and thus allows rapid screening of potential components of QD-based photocatalytic systems.

■ ASSOCIATED CONTENT

Supporting Information

Details of synthesis and characterization of PbS QDs, error analysis, cyclic voltammogram of BQ, 1D NOESY spectrum, determination of K_a, derivation of eq 1, and simulations of μs dynamics. This material is available free of charge via the Internet at http://pubs.acs.org.

■ AUTHOR INFORMATION

Corresponding Author

e-weiss@northwestern.edu

Notes

The authors declare no competing financial interest.

■ ACKNOWLEDGMENTS

This work was supported by a grant from the Air Force Office of Scientific Research (AFOSR, No. FA9550-10-1-0220) through a Young Investigator Award to E.A.W. K.E.K. is supported by the U.S. Department of Energy Office of Science Graduate Fellowship Program (DOE SCGF). The authors thank Dr. Nathan Mathew for assistance with NIR photoluminescence measurements.

■ REFERENCES

(1) Nootz, G.; Padilha, L. A.; Levina, L.; Sukhovatkin, V.; Webster, S.; Brzozowski, L.; Sargent, E. H.; Hagan, D. J.; Van Stryland, E. W. *Phys. Rev. B* **2011**, *83*, 155302.
(2) Nair, G.; Bawendi, M. G. *Phys. Rev. B* **2007**, *76*, 081304.
(3) Nair, G.; Chang, L. Y.; Geyer, S. M.; Bawendi, M. G. *Nano Lett.* **2011**, *11*, 2145.
(4) Clark, S. W.; Harbold, J. M.; Wise, F. W. *J. Phys. Chem. C* **2007**, *111*, 7302.
(5) Gaponenko, M. S.; Lutich, A. A.; Tolstik, N. A.; Onushchenko, A. A.; Malyarevich, A. M.; Petrov, E. P.; Yumashev, K. V. *Phys. Rev. B* **2010**, *82*, 125320.
(6) Zhang, J. M.; Zhang, X. K.; Zhang, J. Y. *J. Phys. Chem. C* **2009**, *113*, 9512.
(7) Sambur, J. B.; Novet, T.; Parkinson, B. A. *Science* **2010**, *330*, 63.
(8) Robel, I.; Kuno, M.; Kamat, P. V. *J. Am. Chem. Soc.* **2007**, *129*, 4136.
(9) Yang, Y.; Rodriguez-Cordoba, W.; Lian, T. Q. *J. Am. Chem. Soc.* **2011**, *133*, 9246.
(10) Hyun, B. R.; Bartnik, A. C.; Lee, J. K.; Imoto, H.; Sun, L. F.; Choi, J. J.; Chujo, Y.; Hanrath, T.; Ober, C. K.; Wise, F. W. *Nano Lett.* **2010**, *10*, 318.
(11) Hines, M. A.; Scholes, G. D. *Adv. Mater.* **2003**, *15*, 1844.
(12) Burda, C.; Green, T. C.; Link, S.; El-Sayed, M. A. *J. Phys. Chem. B* **1999**, *103*, 1783.
(13) Morris-Cohen, A. J.; Donakowski, M. D.; Knowles, K. E.; Weiss, E. A. *J. Phys. Chem. C* **2010**, *114*, 897.
(14) Wehrenberg, B. L.; Guyot-Sionnest, P. *J. Am. Chem. Soc.* **2003**, *125*, 7806.
(15) Malicki, M.; Knowles, K. E.; Weiss, E. A. *Chem. Commun.* **2012**, DOI: 10.1039/C2CC32895J.
(16) Morris-Cohen, A. J.; Frederick, M. T.; Cass, L. C.; Weiss, E. A. *J. Am. Chem. Soc.* **2011**, *133*, 10146.
(17) Morris-Cohen, A. J.; Vasilenko, V.; Amin, V. A.; Reuter, M. G.; Weiss, E. A. *ACS Nano* **2012**, *6*, 557.
(18) Warner, J. H.; Thomsen, E.; Watt, A. R.; Heckenberg, N. R.; Rubinsztein-Dunlop, H. *Nanotechnology* **2005**, *16*, 175.
(19) Lakowicz, J. R. *Principles of Fluorescence Spectroscopy*, 3rd ed.; Springer: New York, 2006.